DOI: 10.1002/chem.201000187

Sonication-Triggered Instantaneous Gel-to-Gel Transformation

Xudong Yu, Qian Liu, Junchen Wu, Mingming Zhang, Xinhua Cao, Song Zhang, Qi Wang, Liming Chen, and Tao Yi*[a]

Abstract: Two new peptide-based isomers containing cholesterol and naphthalic groups have been designed and synthesized. We found that the position of L-alanine in the linker could tune the gelation properties and morphologies. The molecule with the L-alanine residue positioned in the middle of the linker (**1b**) shows better gelation behavior than that with L-alanine directly linked to the naphthalimido moiety (**1a**). As a result, a highly thermostable organogel of **1b** with a unique core–shell structure was obtained at high temperature and pressure in acetonitrile. Moreover, the gels of **1a** and **1b** could undergo an instantaneous gel-to-gel transition triggered by sonication. Ultrasound could break the core–shell microsphere of **1b** and the micelle structure of **1a** into entangled fibers. By studying the mechanism of the sonication-triggered gel-to-gel transition process of these compounds, it can be concluded that ultrasound has a variety of effects on the morphology, such as cutting, knitting, unfolding, homogenizing, and even cross-linking. Typically, ultrasound can cleave and homogenize π-stacking and hydrophobic interactions among the gel molecules and then reshape the morphologies to form a new gel. This mechanism of morphology transformation triggered by sonication might be attractive in the field of material storage and controlled release.

Keywords: gel-to-gel transitions · gels · peptides · self-assembly · sonication

Introduction

Supramolecular assembly through noncovalent interactions such as hydrogen bonding, π–π stacking, van der Waals forces, and hydrophobic and electrostatic interactions has attracted increasing interest for its potential application in biodelivery and separation systems, sensing devices, pollutant capture and removal, gas or medicine storage, and controlled release.[1] It is well-known that crystal, gel, and sol phases are the main studied systems for supramolecular aggregates. Light,[2] sound,[3] pH value,[4] solvent,[5] ions,[6] biomolecules including enzymes,[7] and so forth are usually used as stimuli to tune the behavior of the molecular assembly for functional expression or potential applications. The most reported response processes are sol-to-sol, sol-to-crystal, sol-to-gel, and gel-to-sol transitions, which are often accompanied by spectrum or morphology changes. Recently, direct crystal-to-crystal[8] transformations with assembly changes or mechanical action have become an attractive area of research because these solid-to-solid transformations, which bypass the intermediate sol state, are more convenient for controlled release and for functional expression and engineering. For example, Irie and co-workers reported a reversible and rapid macroscopic crystal-to-crystal change in shape and size based on diarylethene chromophores induced by light.[9] However, the obtainment of single crystals was difficult and random with poor reproducibility. The use of low-molecular-weight gels that undergo reversible dissociation and association to allow deconstruction and reconstruction of their molecular components by noncovalent interactions is attractive due to the dynamic nature of these systems.[10] Those that can be influenced by external stimuli are of particular interest and play a crucial role as functional soft materials.[11] Up to now, few studies of responsive gel-to-gel transformations have been performed with organogels, although there are many reports of responsive gel–sol transitions. However, it must be noted that a gel-to-gel transformation may be more promising for further potential applications.

Ultrasound has been widely used in the food and cosmetic industries and with nanomaterials to disperse particles. Very

[a] X. Yu, Q. Liu, Dr. J. Wu, M. Zhang, X. Cao, S. Zhang, Q. Wang, L. Chen, Prof. T. Yi
Department of Chemistry and Laboratory of Advanced Materials, Fudan University
220 Handan Road, Shanghai 200433 (China)
Fax: (+86) 21-55664621
E-mail: yitao@fudan.edu.cn

Supporting information for this article is available on the WWW under http://dx.doi.org/10.1002/chem.201000187.

recently, ultrasound is also unique in being used both for in vivo molecular imaging and as a therapeutic tool. However, the effect of ultrasound on the self-assembly process of molecules (or biomolecules) is still not clear. In the past few years, ultrasound has begun to play a significant role in the organogel field. It was believed that sonication could cleave self-locked intramolecular hydrogen bonds[12] or π stacking[13] to form interlocked gel states through intermolecular interactions. Very recently, we reported an ultrasound switch and thermal self-repair in a cholesterol-based self-assembly system. The sonocrystallization mechanism in the sol-to-gel process has also been studied elaborately.[14] However, those systems must undergo a sol-to-gel transformation through a heating–cooling process in order to realize gelation by sonication. In the present report, a direct gel-to-gel transformation triggered by sonication was observed and studied. In this case, two new peptide-based compounds, **1a** and **1b**, were designed and synthesized (Scheme 1). It was expected that the position of the L-alanine residue would affect the intermolecular hydrogen bonding involved in the aggregation of the molecules and would thus enable control of the formation of the gel by a specific stimulus. It is exciting that the gel of **1b** from acetonitrile and toluene could undergo instantaneous gel-to-gel transition with shape and size changes when subjected to sonication. To the best of our knowledge, this is the first example of ultrasound-induced aggregation change in a gel system without a sol-to-gel transition.

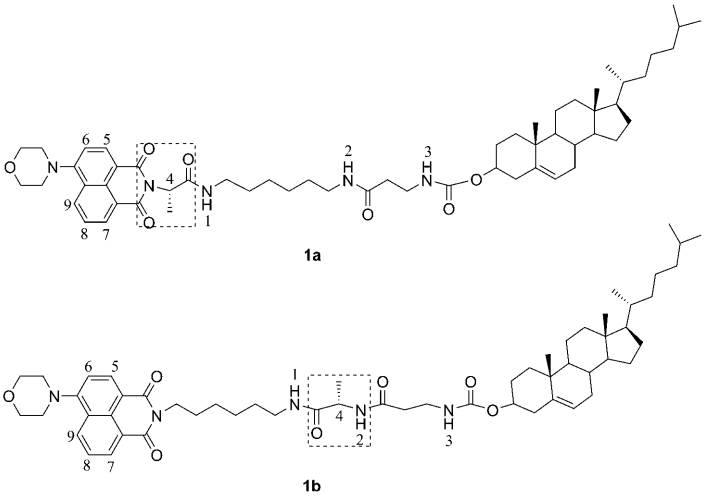

Scheme 1. Chemical structures of **1a** and **1b**. The dotted box indicates the position of the L-alanine moiety.

Results and Discussion

The synthesis and characteristics of **1a** and **1b** are described in the Supporting Information. **1a** and **1b** were excellent gelators that could gelate a series of polar or apolar organic solvents, such as benzene, toluene, acetone, ethyl acetate, ethanol, propanol, and acetonitrile (Table S1 and Figure S1 in the Supporting Information). As a typical example, the gelation behavior of **1a** and **1b** in CH_3CN was studied in detail. **1a** and **1b** could not be dissolved entirely in acetonitrile at normal pressure, even if the acetonitrile was boiling. It was surprising that, in a closed tube with high temperature (above 100 °C) and high pressure, both **1a** and **1b** dissolved. As a result, after cooling to 30 °C, **1a** quickly precipitated in CH_3CN to give an irregular nanomicelle morphology that could be observed by SEM (Figure 1a). However, **1b** formed a highly thermostable gel (T-gel)[15] with a unique core–shell structure (gel-to-sol transition temperature $T_g = 104$ °C, > boiling point of acetonitrile; 25 mg mL^{-1}). A dense core of about 2 μm in diameter with a floppy surrounding layer formed by entangled fibers was seen in the SEM, TEM, and CLSM images (Figure 1b, c,

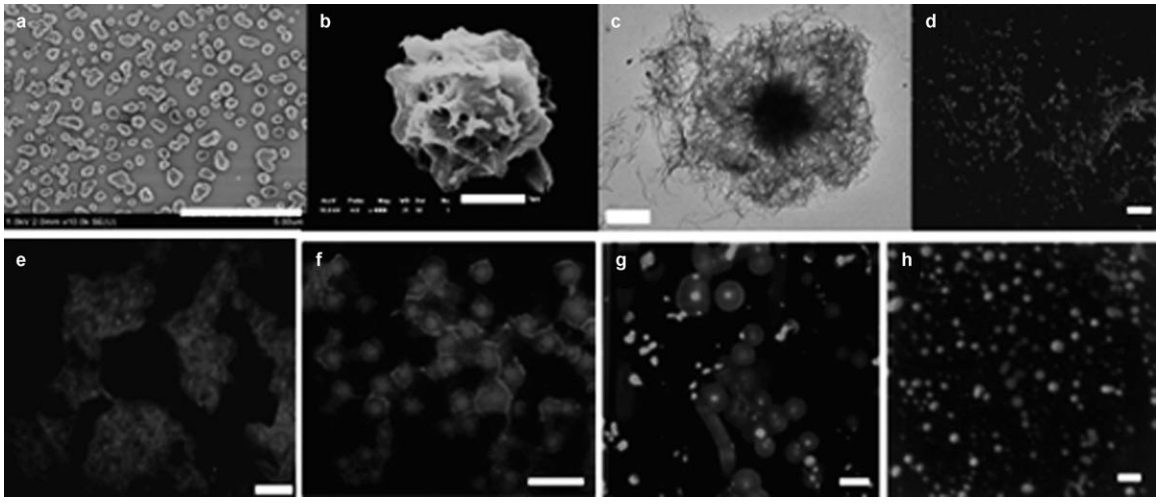

Figure 1. SEM images of a) the **1a** precipitate and b) the **1b** T-gel. TEM image of c) the **1b** T-gel. Confocal laser scanning microscopy (CLSM) images of the **1b** T-gel at d) 55, e) 40, and f) 30 °C at 25 mg mL^{-1}; g) of the **1b** T-gel at 12.5 mg mL^{-1}, and h) of the suspension at 7.5 mg mL^{-1} at 30 °C. Scale bars: a) 5, b) 5, c) 2, d) 50, e) 100, f) 20, g) 5, and h) 2 μm.

and f). To further investigate the core–shell structure of the **1b** T-gel, the dynamic process in the gels was followed upon cooling from 120 °C to 55, 40, and 30 °C, respectively, by means of CLSM. The experiments show that 1) instantaneous nucleation occurred as the balls formed and fibers grew on the surface of the balls at 55 °C (Figure 1 d), 2) then the fibers grew out from the balls and entangled with each other at 40 °C (Figure 1 e), and 3) finally, a distinct net structure wrapping the balls was obtained at 30 °C (Figure 1 f). The concentration-dependent morphology evolution of the **1b** gels also confirmed the same mechanism. In a less concentrated **1b** T-gel at $c = 12.5\ mg\,mL^{-1}$ (critical gel concentration, CGC), both core–shell balls and spheres were observed by CLSM (Figure 1 g). However, in a suspension with a lower concentration than the CGC, for example, $7.5\ mg\,mL^{-1}$, only spheres were observed (Figure 1 h). These results indicated that the **1b** molecules were inclined to form a spherical structure in the initial stage of the thermal process. This morphology formed at high pressure and temperature was just like the porous polymeric microspheres fabricated through a new solid-in-oil-in-water (S/O/W) emulsion technique.[16]

Interestingly, both **1a** and **1b** could form gels when subjected to sonication (S-gels). The morphology of **1a** underwent transition from micelles to tightly arranged entangled fibers when the molecules were subjected to sonication (2 min, $0.37\ W\,cm^{-2}$, 40 KHz) in the temperature range of 50–70 °C (Figure 2 a–c). It should be noted that no gelation occurred when the temperature was lower than 50 °C, which meant that the precipitate could not directly transform into a gel upon ultrasound treatment at lower temperatures. On the other hand, **1b** underwent a gel-to-gel transformation in the temperature range of 30–70 °C. SEM images indicated that a structural change from core–shell to entangled nanofibers happened when the **1b** T-gel was subjected to sonication (Figure 2 g–l). At 30 °C, besides the entangled fibers and cross-linked nanoballs, a few distinct nanoballs could also be seen in some areas in the S-gel (Figure 2 j), whereas at a temperature higher than 40 °C, large areas of only entangled fibers were observed by SEM (Figure 2 k,l). To further understand the impact of sonication on the core–shell structure in the T-gel, time-dependent sonication experiments were carried out (Figure 3). When **1b** was subjected to sonication for 30–180 s, the entangled fibers around the shell were stretched and incised, and the microball at the inner core was cut into nanoballs and then released. Most importantly, the dispersed nanoballs could further assemble into cross-linked fibers. Simultaneously, this

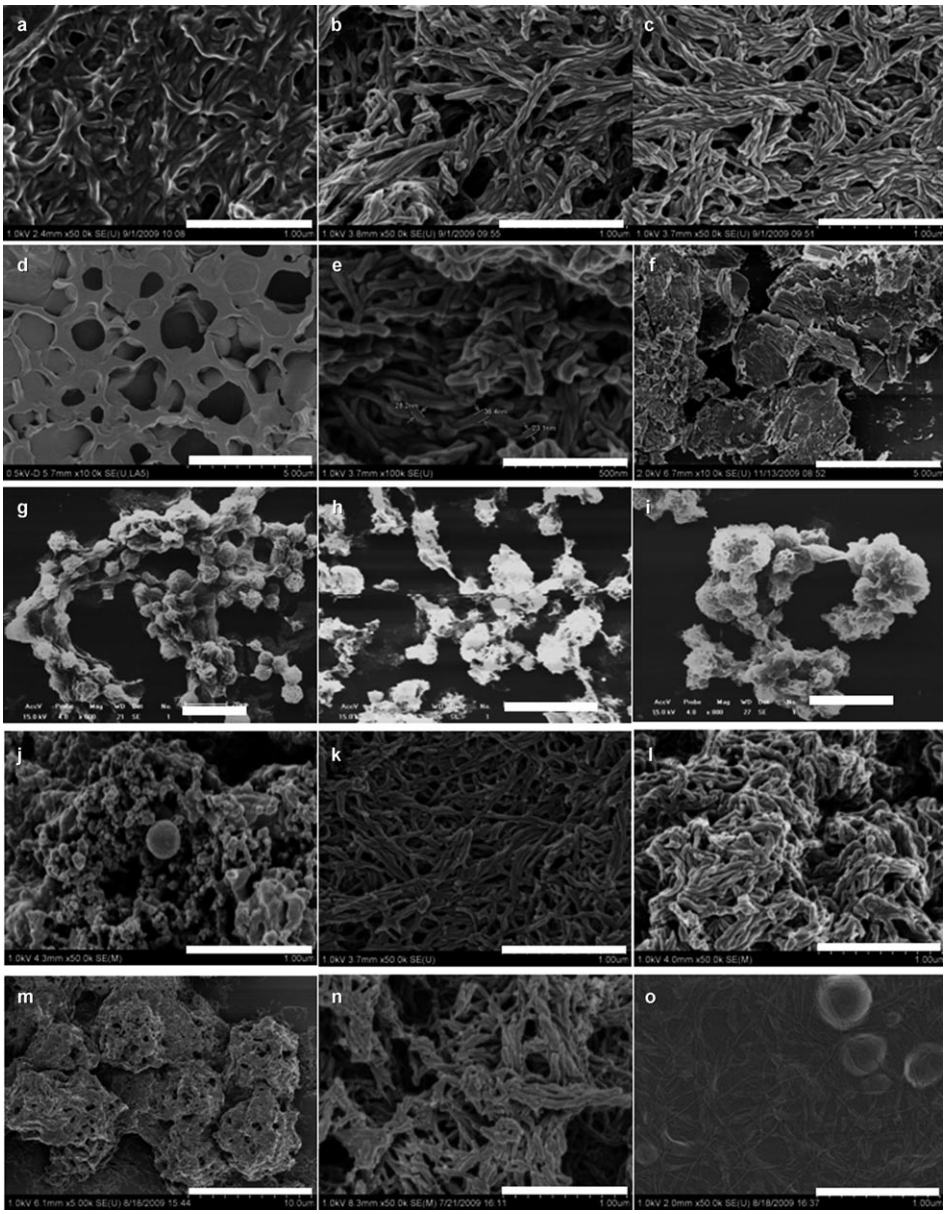

Figure 2. SEM images of the **1a** S-gels at temperatures of a) 50, b) 60, and c) 70 °C, of the **1a** TS-gels at temperatures of d) 30, e) 40, and f) 70 °C, and of the **1b** T-gels (g–i), S-gels (j–l), and TS-gels (m–o) at temperatures of 30, 40, and 70 °C (from left to right, respectively). All gels in acetonitrile at a concentration of $25\ mg\,mL^{-1}$. Scale bars: a–c, j–l, n, and o) 1 μm, d) 5 μm, e) 500 nm, f) 5 μm, g–i) 20 μm; m) 10 μm.

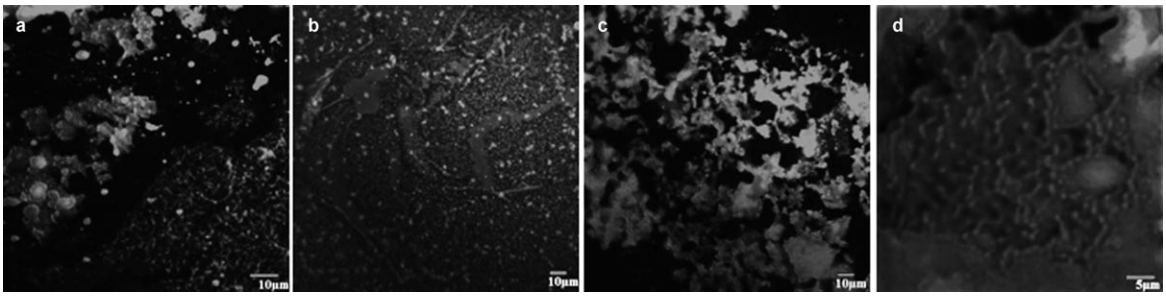

Figure 3. CLSM images of T-gels of **1b** from acetonitrile subjected to sonication for a) 30, b) 90, c) 120, or d) 180 s. Scale bars: 10, 10, 10, and 5 μm for a–d, respectively.

process of breaking down and then fitting together was accompanied by a rapid gel to partial gel (P-gel) to gel transformation (within several seconds) without a temperature change. The mechanism of this process might be useful for the design and synthesis of new nanomaterials through the use of ultrasound. Furthermore, toluene, as an apolar solvent, was also employed for gelation. Both **1a** and **1b** could form transparent gels in toluene and underwent gel-to-gel transformation when subjected to ultrasound. The SEM images revealed that a bundle structure of the T-gel of **1a** was knitted into a hexagonally shaped structure after sonication for 120 s at 40 °C. On the other hand, fibers of the T-gel of **1b** with a width of about 100 nm were cut into spindly fibers with widths of 20–40 nm in toluene (Figure 4).

For comparison, the traditional sol–gel process of gel formation from CH_3CN triggered by sonication was also studied. In this process, the sample was heated to form the sol state at 120 °C and then quickly put into a thermostat at a certain temperature and subjected to sonication (2 min). The gel was called a TS-gel. These TS-gels showed different morphologies that were cooperatively controlled by heat and sound. By this sol–gel process, **1a** instantly formed opaque TS-gels in the range from 30 to 70 °C. The SEM images revealed a net structure at 30 °C (Figure 2 d), nanofibers at 40 °C (Figure 2 e), and layer structures at 60 and 70 °C (Figure 2 f) for **1a**, whereas **1b** showed a cotton-like structure at 30 °C (Figure 2 m), nanofibers at 40 °C (Figure 2 n), and fibers and balls at 60 and 70 °C (Figure 2 o). It should be noted that below 40 °C the morphologies of both the **1a** and **1b** TS-gels were similar to those of the S-gels. In a typical thermal process, the gelling time becomes longer with an increase in the temperature of the thermostat, from 24 s at 30 °C to 56 s at 70 °C for **1b** to form a T-gel. Therefore, a competition between the effect of sonication and the thermal process existed in the formation of the TS-gel. At lower temperatures, the system lacks enough time to keep the sol state; the so-called TS-gel is, in principle, an S-gel. These experiments testified that the formation of ultrasound-induced fibers needs enough energy to overcome a high energy barrier.[3,17] A force balance involving the thermal and ultrasound treatments operates on the various morphologies of the gels, so a proper temperature is important to obtain the desired gel. Table 1 indicates the different states of **1a** and **1b** and the effect of temperature changes in the thermal, ultrasound, and thermal–ultrasound processes. It was noted that sonication as a stimulus enlarged the gelation temperature range. Moreover, compared with those TS-gels obtained by the sol–gel process, S-gels obtained by the gel-to-gel process were more homogeneous and stable, with very little sonocrystallization, especially at higher temperatures.

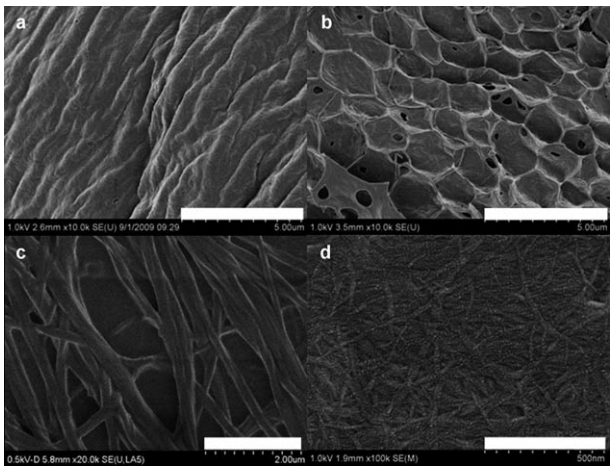

Figure 4. SEM images of **1a** and **1b** gels formed at 40 °C in toluene: a) **1a** T-gel, b) **1a** S-gel, c) **1b** T-gel, and d) **1b** S-gel. Scale bars: a, b) 5 μm, c) 2 μm, and d) 500 nm.

Table 1. Different states of **1a** and **1b** treated with various processes in CH_3CN.[a]

Process	Sample	Temperature [°C]						
		30	40	50	55	60	70	75
thermal[b]	**1a**	P	P	P	P	P	P	P
	1b	G	G	G	G	PG	PG	PG
sonication[c]	**1a**	P	P	G	G	G	G	PG
	1b	G	G	G	G	G	G	PG
T-S[d]	**1a**	G	G	G	G	G	G	PG
	1b	G	G	G	G	G	G	PG

[a] The concentration of all of the gels was 25 mg mL^{-1}. G: gel; PG: partial gel; P: precipitation. [b] Heated to 120 °C, cooled to a certain temperature, and aged for at least 40 min. [c] Gel samples directly treated with ultrasound for 120 s (0.37 W cm^{-2}, 40 KHz). [d] T-gel heated to 120 °C, quickly cooled to a certain temperature, and subjected to sonication.

The temperature-dependent NMR data of the gels indicated that hydrogen bonding between the amide moieties participated in the self-assembly (Figure 5). The signals of

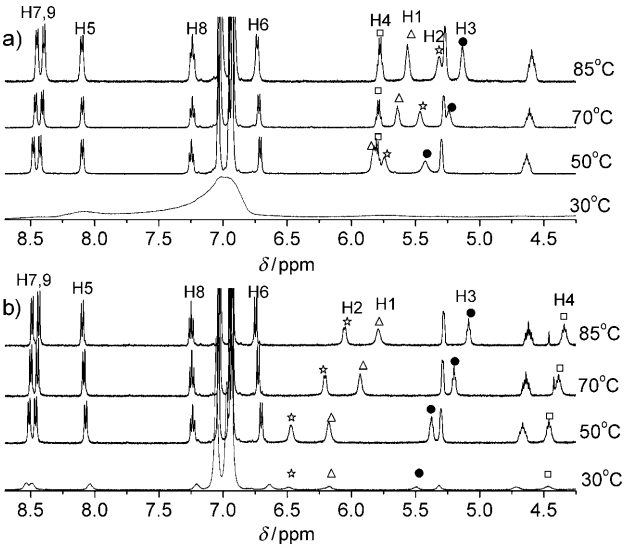

Figure 5. Temperature-dependent ^{1}H NMR spectra of T-gels of a) **1a** and b) **1b** from toluene (25 mg mL^{-1}). The positions of the labeled protons are marked in Scheme 1.

the amide protons NH1, NH2, and NH3 of the **1b** T-gel in toluene (25 mg mL^{-1}) shifted upfield from $\delta = 6.49$ to 6.05, 6.17 to 5.80, and 5.49 to 5.09 ppm, respectively, between 30 and 85 °C. The signals from the thermal dissociation process for the **1b** S-gel in toluene showed similar changes to those for the T-gel; for example, the signals of NH1, NH2, and NH3 shifted from $\delta = 6.52$ to 6.07, 6.20 to 5.80, and 5.51 to 5.09 ppm, respectively, between 30 and 85 °C. The methine proton (H4) of the L-alanine group was also obviously shifted upfield from $\delta = 4.47$ to 4.34 ppm, whereas the protons in the naphthalic group (H5 and H6) showed slightly downfield shifts with an increase in temperature. The **1a** gel exhibits almost no signals at room temperature because of aggregation. In the process of the gel-to-sol transformation of **1a**, the signals of the amide protons were also shifted upfield; however, the $\Delta\delta$ value between 50 and 85 °C for H1 in **1a** (0.25 ppm) is obviously smaller than that in **1b** (0.38 ppm). The signals for the protons on the methine (H4) and naphthalic groups in **1a** show almost no shift with the temperature change. The above result indicated that intermolecular hydrogen bonding of the peptide, as well as π–π stacking, play a much more important role in the self-assembly of the molecules in **1b** than in **1a**.

The infrared spectra of **1a** and **1b** also confirmed the contribution of hydrogen bonds between amide groups to the gelation. A comparison of the IR spectra in the N–H and C=O stretching range indicated the formation of much stronger H-bonds in the gels of **1b** than those of **1a** (Table 2). The N–H stretching bands (ν_{NH}) of **1b** in both the T-gel and the S-gel from CH_3CN were positioned at

Table 2. The wavenumbers of the IR band related to H-bonding and the maximum emission peaks in the fluorescence spectra.[a]

Sample	Solvent	State	ν [cm^{-1}]	λ_{em}-G [nm]	λ_{em}-S [nm]
1a	acetonitrile	precipitate[b]	3361, 1698, 1655	536	551
		S-gel[b]	3351, 1689, 1648	531	
	toluene	T-gel	3302, 1690, 1647	507[c]	507
		S-gel	3306, 1689, 1655	509[c]	
1b	acetonitrile	T-gel[c]	3287, 1693, 1651	531	530
		S-gel[c]	3281, 1686, 1649	530	
	toluene	T-gel	3285, 1690, 1650	522[c]	502
		S-gel	3283, 1690, 1651	517[c]	

[a] G: gel; S: solution. Performed at room temperature unless otherwise stated. [b] Performed at 50 °C. [c] Performed at 30 °C.

3289 cm^{-1} at room temperature (20 °C; see the Supporting Information). However, at 30 °C, this ν_{NH} band moved from 3287 cm^{-1} in the T-gel to 3281 cm^{-1} in the S-gel, which indicated the formation of much stronger hydrogen bonding after the sonication. Ultrasound also enhanced the hydrogen bonding of **1b** in toluene, so that the N–H stretching band (ν_{NH}) of 3285 cm^{-1} in the T-gel changed to 3283 cm^{-1} in the S-gel. The ν_{NH} band at 3360 cm^{-1} for **1a** powder (from CH_3CN) changed to 3353 cm^{-1} in the S-gel at room temperature. At 50 °C, this ν_{NH} band moved from 3361 cm^{-1} in the T-gel to 3351 cm^{-1} in the S-gel, which also suggested strengthened hydrogen bonding after sonication. By contrast, the ν_{NH} band shifted from 3302 to 3306 cm^{-1} during the transformation from the T-gel of **1a** to the S-gel in toluene. From these results, it could be ascertained that sonication does not always result in the breakage of hydrogen bonding. The fluorescence spectra of **1b** in CH_3CN (λ_{em}: 530 nm) show almost no change from the solution to the gel states at 30 °C (see the Supporting Information) but displayed redshifts of about 20 and 15 nm in toluene from dilute solution to the T-gel and the S-gel, respectively. However, the emission band of **1a** in acetonitrile blueshifted from 551 nm in dilute solution to 536 and 531 nm in the powder and the S-gel, respectively, at 50 °C. The above result meant that intermolecular π–π stacking was not a primary factor in the formation of a T-gel in the present system. However, the result shows that π–π stacking can be tuned by sonication to some extent, as can be seen from a comparison of the emission spectra of the S-gel and the T-gel of **1b** in toluene or powder and the S-gel of **1a** in acetonitrile (Table 2).

To gain a deeper insight into the assembly mechanism, small-angle X-ray scattering (SAXS), powder X-ray diffraction (XRD), and water contact-angle (CA) experiments were also carried out. The XRD signal (see the Supporting Information, Figure S15–17) of the **1b** xerogel from toluene

gave peaks at 5.35 and 2.63 nm with a ratio of 2:1, which indicates a lamellar structure. The distance of 5.35 nm was close to twice the length of the bent molecular distance of **1b**, which suggested that the aggregates formed as a bilayer structure. The broad and weak peak of the S-gel in toluene revealed a more disordered structure. On the other hand, the SAXS data of gels of **1b** in acetonitrile showed weak peaks at 5.92 nm, which indicated a different structure than that found in toluene gels. Moreover, the CA experiments (Figure 6) revealed that the xerogel of **1b** from acetonitrile had a superhydrophobic surface with CA = 151.2°; this value decreased when the gel was subjected to sonication (S-gel with CA = 127.8°), possibly due to nanopores on the rough surface of the T-gel trapping air to greatly increase hydrophobicity, according to the modified Cassie equation.[18] By contrast, the xerogel of **1b** from toluene had a more hydrophilic surface (CA = 92.7°). From these results, a gelation mechanism was proposed (Figure 7). Before self-assembly, **1b** has a U-shaped structural conformation caused by weak intramolecular interactions between the naphthalimide and cholesterol groups in acetonitrile. The U-shaped molecules favored the formation of dimers by strong intermolecular hydrogen bonding. In the gel state, the dimers aggregated by hydrophobic interactions to form a core–shell structure, which can be tuned by sonication into entangled fibers. In toluene, the solvophilic effect between toluene and the naphthalimide group of **1b** makes the molecule adapt a V-shaped conformation and then self-assemble into a lamellar structure by hydrogen bonding, hydrophobic interactions, and weak π–π interactions. Sonication weakens the latter two intermolecular interactions and thus results in much tinier fibril structures.

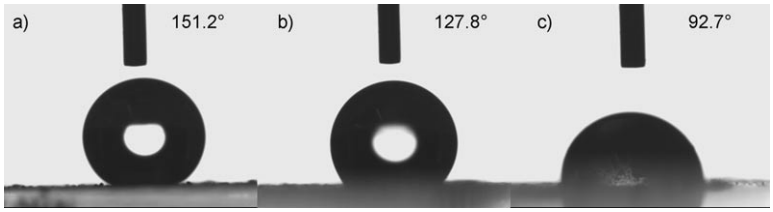

Figure 6. Photographs of water droplets on glass slides spin-coated with **1b** xerogels: a) T-gel from acetonitrile, b) S-gel from acetonitrile, and c) T-gel from toluene.

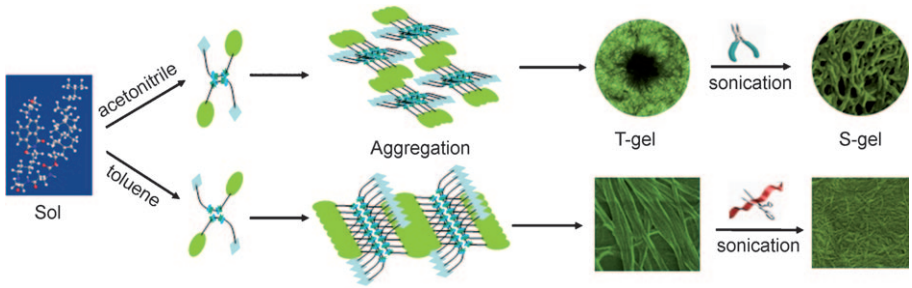

Figure 7. Schematic representation of the aggregation changes of **1b** in acetonitrile and toluene.

The high thermostability of the **1a** and **1b** gels in acetonitrile was taken into consideration when the stability of the gels in water was checked. The T-gel of **1b** in acetonitrile (25 mg mL^{-1} with 200 μL of acetonitrile) was treated with water (300 μL) on the surface of the gel (see images in the Supporting Information). After one week, the interface between the gel and water was still well defined. Moreover, the gel was maintained when the tube was reversed. However, some bubbles appeared in the aqueous phase and the water color changed from clear to pale yellow. This suggested a chemical exchange between the aqueous and gel phases. We assumed that a small amount of water penetrated into the gel network, accompanied by the acetonitrile solution of the gelator transitioning into the aqueous phase, to give a pale yellow color. This result is favorable for the application of these gels in drug-delivery systems; further work is under progress in our laboratory.

Conclusion

This work presents two new methods for gel preparation: gel production under high pressure and a gel-to-gel transformation process triggered by ultrasound treatment. A highly thermostable organogel with a unique core–shell structure was obtained at higher temperature and pressure, and ultrasound could break these core–shell microspheres into nanoballs under mild conditions. Most importantly, the nanoballs could be fractured and further cross-linked between themselves into entangled fibers through hydrophobic interactions on the surface when subjected to sonication. Furthermore, the sonication-induced S-gel has higher thermostability. After studying the mechanism of the sonication-triggered instant gel-to-gel transition process of **1a** and **1b** gels from acetonitrile and toluene, we propose that ultrasound does not cleave intermolecular hydrogen bonding in the peptide system but can truncate and homogenize the π-stacking and hydrophobic interactions among the gel molecules and then change the morphologies to ones more favorable for gelation. This research provides a good example for understanding how sonication influences the self-assembly process of molecular systems containing peptides. This morphology transformation triggered by sonication might be applicable in controlled release and for responsive and shape-memory materials.

Experimental Section

General: All starting materials were obtained from commercial supplies and used as received. Di-*tert*-butyldicarbonate (97%) was provided from Alfa Aesar. Dicyclohexylcarbodiimide (DCC; 99%) was obtained from Acros. Cholesteryl chloroformate (99%) was obtained from Fluka. Morpholine (CP), L-alanine (98.5%), 4-bromo-1,8-naphthalic anhydride (95%), and hexane-1,6-diamine (CP) were supplied from Sinopharm Chemical Reagent Co., Ltd. (Shanghai). ^{1}H and ^{13}C NMR spectra were recorded on a Mercuryplus instrument, at 400 and 100 Hz, respectively. Temperature-dependent ^{1}H NMR spectra were recorded by using a Bruker DMX 500 spectrometer at 500 Hz. MALDI-TOF MS was performed on an Auto FLEX III MALDI-TOF mass spectroscopy instrument (Bruker Daltonics Inc.). ESI-MS data were recorded on a Waters Quattro Micro API LC-MS-MS spectrometer (Waters, USA). Elemental analysis was carried out on a VARIOEL3 apparatus (ELEMENTAR). Melting points were determined on an XT4-100A hot-plate melting point apparatus without correction.

The gelation test: The gelation tests on **1a** and **1b** were carried out with various solvents by using a test-tube-inversion method.[19] The tube was heated to 120°C and then put into a thermostat controlled by water. A T-gel was obtained when the prepared sample was left for a period of time in a certain solvent and at a certain temperature. An S-gel was obtained by direct ultrasonic treatment (0.37 W cm^{-2}, 40 KHz) of the prepared T-gel for 120 s at a certain temperature, whereas a TS-gel was prepared after a T-gel was heated to the sol state and then quickly put into a thermostat at a certain temperature and subjected to sonication for 120 s.

Techniques: FTIR spectra were recorded by using an IRPRESTIGE-21 spectrometer (Shimadzu). SEM images of the xerogels were obtained by using SSX-550 (Shimadzu) and FE-SEM S-4800 (Hitachi) instruments. Samples were prepared by spinning the gels on glass slides, freeze-drying them, and coating them with Au. TEM was performed on a JEOL JEM2011 apparatus operating at 200 kV. The samples were prepared by putting the gel on a carbon-coated copper grid and freeze-drying it for 48 h. SAXS experiments were carried out on a Nanostar U SAXS system (Bruker) at room temperature. The X-ray diffraction pattern was generated by using a Bruker AXS D8 instrument (Cu target; $\lambda = 0.1542$ nm) with a power of 40 kV and 50 mA. Contact-angle measurements were performed by using the sessile-drop method (Dataphysics, OCA 20). The water droplets were introduced with a microsyringe, and images were captured to measure the angle of the liquid–solid interface. CLSM experiments were performed on an Olympus IX81 confocal laser scanning microscope equipped with a 60× oil-immersion objective lens. Excitation at 405 nm was carried out with a semiconductor laser. Emission was collected between 450 and 550 nm. An organogel spot was prepared on a dish for CLSM observation. Sonication treatment of a sol was performed in a KQ-500DB ultrasonic cleaner (maximum power, 100 W, 40 KHz, Kunshang Ultrasound Instrument Co, Ltd., China).

Acknowledgements

This work was supported by the National Science Foundation of China (20771027, 30890141), the National Basic Research Program of China (2009CB930400), the Specialized Research Fund for the Doctoral Program of Higher Education (200802460007), Shanghai Sci. Tech. Comm. (08JC1402400), and the Shanghai Leading Academic Discipline Project (B108).

[1] a) P. Terech, R. G. Weiss, *Chem. Rev.* **1997**, *97*, 3133–3159; b) J. E. G. J. Wijnhoven, W. L. Vos, *Science* **1998**, *281*, 802–804; c) B. T. Holland, C. F. Blanford, A. Stein, *Science* **1998**, *281*, 538–540; d) J. F. Miravet, B. Escuder, *Org. Lett.* **2005**, *7*, 4791–4794; e) S. Kiyonaka, K. Sugiyasu, S. Shinkai, I. Hamachi, *J. Am. Chem. Soc.* **2002**, *124*, 10954–10955; f) Z. Yang, B. Xu, *J. Mater. Chem.* **2007**, *17*, 2385–2393; g) N. M. Sangeetha, U. Maitra, *Chem. Soc. Rev.* **2005**, *34*, 821–836.

[2] a) O. J. Dautel, M. Robitzer, J. P. Lère-Porte, F. Serein-Spirau, J. J. E. Moreau, *J. Am. Chem. Soc.* **2006**, *128*, 16213–16223; b) N. Koumura, M. Kudo, N. Tamaoki, *Langmuir* **2004**, *20*, 9897–9900; c) N. Fujita, Y. Sakamoto, M. Shirakawa, M. Ojima, A. Fujii, M. Ozaki, S. Shinkai, *J. Am. Chem. Soc.* **2007**, *129*, 4134–4135; d) P. C. Xue, R. Lu, G. J. Chen, Y. Zhang, H. Nomoto, M. Takafuji, H. Ihara, *Chem. Eur. J.* **2007**, *13*, 8231–8239; e) S. Z. Xiao, Y. Zou, M. X. Yu, T. Yi, Y. F. Zhou, F. Y. Li, C. H. Huang, *Chem. Commun.* **2007**, 4758–4760; f) S. Wang, W. Shen, Y. L. Feng, H. Tian, *Chem. Commun.* **2006**, 1497–1499; g) J. J. D. de Jong, L. N. Lucas, R. M. Kellogg, J. H. van Esch, B. L. Feringa, *Science* **2004**, *304*, 278–281.

[3] a) D. Bardelang, *Soft Matter* **2009**, *5*, 1969–1971; b) G. Cravotto, P. Cintas, *Chem. Soc. Rev.* **2009**, *38*, 2684–2697.

[4] a) A. Aggeli, M. Bell, N. Boden, J. N. Keen, P. F. Knowles, T. C. B. McLeish, M. Pitkeathly, S. E. Radford, *Nature* **1997**, *386*, 259–262; b) S. L. Zhou, S. Matsumoto, H. D. Tian, H. Yamane, A. Ojida, S. Kiyonaka, I. Hamachi, *Chem. Eur. J.* **2005**, *11*, 1130–1136.

[5] a) W. Cai, G. T. Wang, Y. X. Xu, X. K. Jiang, Z. T. Li, *J. Am. Chem. Soc.* **2008**, *130*, 6936–6937; b) Y. Zhou, T. Yi, T. Li, Z. Zhou, F. Li, W. Huang, C. Huang, *Chem. Mater.* **2006**, *18*, 2974–2981.

[6] a) J. K. H. Hui, Z. Yu, T. Mirfakhrai, M. J. MacLachlan, *Chem. Eur. J.* **2009**, *15*, 13456–13465; b) G. O. Lloyd, J. W. Steed, *Nat. Chem. Biol.* **2009**, *5*, 437–442; c) H. Maeda, *Chem. Eur. J.* **2008**, *14*, 11274–11282; d) A. Ajayaghosh, P. Chithra, R. Varghese, *Angew. Chem.* **2007**, *119*, 234–237; *Angew. Chem. Int. Ed.* **2007**, *46*, 230–233; e) A. Ajayaghosh, P. Chithra, R. Varghese, K. P. Divya, *Chem. Commun.* **2008**, 969–971; f) H. Yang, T. Yi, Z. Zhou, Y. Zhou, J. Wu, M. Xu, F. Li, C. Huang, *Langmuir* **2007**, *23*, 8224–8230; g) H.-J. Kim, J.-H. Lee, M. Lee, *Angew. Chem.* **2005**, *117*, 5960–5964; *Angew. Chem. Int. Ed.* **2005**, *44*, 5810–5814.

[7] a) Z. Yang, G. Liang, L. Wang, B. Xu, *J. Am. Chem. Soc.* **2006**, *128*, 3038–3043; b) J. Gao, H. M. Wang, L. Wang, J. Y. Wang, D. L. Kong, Z. M. Yang, *J. Am. Chem. Soc.* **2009**, *131*, 11286–11287; c) F. Zhao, M. L. Ma, B. Xu, *Chem. Soc. Rev.* **2009**, *38*, 883–891.

[8] a) T. H. Kim, Y. W. Shin, J. H. Jung, J. S. Kim, J. Kim, *Angew. Chem.* **2008**, *120*, 697–700; *Angew. Chem. Int. Ed.* **2008**, *47*, 685–688; b) Z. M. Duan, Y. Zhang, B. Zhang, D. B. Zhu, *J. Am. Chem. Soc.* **2009**, *131*, 6934–6935; c) A. K. Sah, T. Tanase, *Chem. Commun.* **2005**, 5980–5981.

[9] S. Kobatake, S. Takami, H. Muto, T. Ishikawa, M. Irie, *Nature* **2007**, *446*, 778–781.

[10] a) P. Cordier, F. Tournilhac, C. Soulié-Ziakovic, L. Leibler, *Nature* **2008**, *451*, 977–980; b) R. P. Sijbesma, F. H. Beijer, L. Brunsveld, B. J. B. Folmer, J. H. K. Hirschberg, R. F. M. Lange, J. K. L. Lowe, E. W. Meijer, *Science* **1997**, *278*, 1601–1604; c) L. A. Estroff, A. D. Hamilton, *Chem. Rev.* **2004**, *104*, 1201–1218; d) K. J. C. van Bommel, A. Friggeri, S. Shinkai, *Angew. Chem.* **2003**, *115*, 1010–1030; *Angew. Chem. Int. Ed.* **2003**, *42*, 980–999; e) J. M. Lehn, *Chem. Soc. Rev.* **2007**, *36*, 151–160.

[11] a) D. J. Abdallah, R. G. Weiss, *Adv. Mater.* **2000**, *12*, 1237–1247; b) J. H. Van Esch, B. L. Feringa, *Angew. Chem.* **2000**, *112*, 2351–2354; *Angew. Chem. Int. Ed.* **2000**, *39*, 2263–2266; c) S. Yagai, T. Nakajima, K. Kishikawa, S. Kohmoto, T. Karatsu, A. Kitamura, *J. Am. Chem. Soc.* **2005**, *127*, 11134–11139; d) A. R. Hurst, D. K. Smith, K. P. Harrington, *Chem. Eur. J.* **2005**, *11*, 6552–6559.

[12] a) J. C. Wu, T. Yi, T. M. Shu, M. X. Yu, Z. G. Zhou, M. Xu, Y. F. Zhou, H. J. Zhang, J. T. Han, F. Y. Li, C. H. Huang, *Angew. Chem.* **2008**, *120*, 1079–1083; *Angew. Chem. Int. Ed.* **2008**, *47*, 1063–1067; b) K. Isozaki, H. Takaya, T. Naota, *Angew. Chem.* **2007**, *119*, 2913–2915; *Angew. Chem. Int. Ed.* **2007**, *46*, 2855–2857; c) Y. Wang, C. Zhan, H. Fu, X. Li, X. Sheng, Y. Zhao, D. Xiao, Y. Ma, J. S. Ma, J. Yao, *Langmuir* **2008**, *24*, 7635–7638.

[13] a) T. Naota, H. Koori, *J. Am. Chem. Soc.* **2005**, *127*, 9324–9325; b) J. M. J. Paulusse, R. P. Sijbesma, *Angew. Chem.* **2006**, *118*, 2392–2396; *Angew. Chem. Int. Ed.* **2006**, *45*, 2334–2337; c) C. Wang, D. Q. Zhang, D. B. Zhu, *J. Am. Chem. Soc.* **2005**, *127*, 16372–16373.

[14] J. C. Wu, T. Yi, Q. Xia, Y. Zou, F. Liu, J. Dong, T. M. Shu, F. Y. Li, C. H. Huang, *Chem. Eur. J.* **2009**, *15*, 6234–6243.
[15] J. Makarević, M. Jokić, L. Frkaneć, D, Katalenić, M. Žinić, *Chem. Commun.* **2002**, 2238–2239.
[16] C. Takai, T. Hotta, S. Shiozaki, Y. Boonsongrit, H. Abe, *Chem. Commun.* **2009**, 5533–5535.
[17] I. A. Coates, D. K. Smith, *Chem. Eur. J.* **2009**, *15*, 6340–6344.
[18] a) A. B. D. Cassie, S. Baxter, *Trans. Faraday Soc.* **1944**, *40*, 546–561; b) T. Sun, L. Feng, X. F. Gao, L. Jiang, *Acc. Chem. Res.* **2005**, *38*, 644–652; c) L. Feng, S. H. Li, Y. S. Li, H. J. Li, L. J. Zhang, J. Zhai, Y. L. Song, B. Q. Liu, L. Jiang, D. B. Zhu, *Adv. Mater.* **2002**, *14*, 1857–1860.
[19] K. Murata, M. Aoki, T. Suzuki, T. Harada, H. Kawabata, T. Komori, F. Ohseto, K. Ueda, S. Shinkai, *J. Am. Chem. Soc.* **1994**, *116*, 6664–6676.

Received: January 23, 2010
Published online: June 22, 2010

